

Determining efficient temperature sets for the simulated tempering method

A. Valentim, M. G. E. da Luz

Departamento de Física, Universidade Federal do Paraná, CP 19044, 81531-980 Curitiba-PR, Brazil

Carlos E. Fiore

*Instituto de Física, Universidade de São Paulo,
Caixa Postal 66318*

05315-970 São Paulo, São Paulo, Brazil

(Dated: September 1, 2014)

In statistical physics, the efficiency of tempering approaches strongly depends on ingredients such as the number of replicas R , reliable determination of weight factors and the set of used temperatures, $\mathcal{T}_R = \{T_1, T_2, \dots, T_R\}$. For the simulated tempering (ST) in particular – useful due to its generality and conceptual simplicity – the latter aspect (closely related to the actual R) may be a key issue in problems displaying metastability and trapping in certain regions of the phase space. To determine \mathcal{T}_R 's leading to accurate thermodynamics estimates and still trying to minimize the simulation computational time, here it is considered a fixed exchange frequency scheme for the ST. From the temperature of interest T_1 , successive T 's are chosen so that the exchange frequency between any adjacent pair T_r and T_{r+1} has a same value f . By varying the f 's and analyzing the \mathcal{T}_R 's through relatively inexpensive tests (e.g., time decay toward the steady regime), an optimal situation in which the simulations visit much faster and more uniformly the relevant portions of the phase space is determined. As illustrations, the proposal is applied to three lattice models, BEG, Bell-Lavis, and Potts, in the hard case of extreme first-order phase transitions, always giving very good results, even for $R = 3$. Also, comparisons with other protocols (constant entropy and arithmetic progression) to choose the set \mathcal{T}_R are undertaken. The fixed exchange frequency method is found to be consistently superior, specially for small R 's. Finally, distinct instances where the prescription could be helpful (in second-order transitions and for the parallel tempering approach) are briefly discussed.

PACS numbers: 05.10.Ln, 05.70.Fh, 05.50.+q

I. INTRODUCTION

Keystone in the study of statistical physics problems, numerical methods are generally expected to fulfil two requirements: (i) first (and surely the most important), to yield precise estimates for the thermodynamical quantities analyzed; (ii) second, to be as simple and as fast as possible in their implementations.

Nevertheless, often the mentioned two requisites strike out in opposite directions. Indeed, consider, e.g., systems in the regime of phase transitions whose distinct regions of the phase space are separated by large free-energy barriers. It is a common situation not only for complex problems like spin glasses, protein folding, and biomolecules conformation [1–5], but also in lattice gas models displaying first-order phase transitions [6, 7]. In all such examples there may be the occurrence of metastability [6, 7]. Thus, when simulated, these systems can get trapped into local minima. Ways to circumvent this technical difficulty should demand more sophisticated evolution dynamics procedures and longer computational times.

Different proposals like, (a) cluster [8], (b) multicanonical [9], (c) Wang-Landau [10], and (d) tempering [11, 12], among others, are relevant algorithms trying to maintain a good balance between features (i) and (ii) above. In special, (d) above relies on the straightforward idea of “heating up” the system to higher temperatures, so to help it to cross the barriers at low temperatures. Moreover, tempering methods have attracted large interest

due to their generality with a broad applicability [13].

There are two major formulations for the tempering approach, namely, parallel (PT) [11] and simulated (ST) [12], where always the start point is to choose a set of R distinct temperatures (with $T_r < T_{r+1}$, $r = 1, \dots, R-1$), $\mathcal{T}_R = \{T_1, T_2, \dots, T_R\}$, in which T_1 is the one of interest. In the PT, configurations from the distinct R replicas (running in parallel) at the different T 's are exchanged. For the ST, a single realization undergoes many temperature changes (among the T 's in \mathcal{T}_R). Thus, the temperature itself is a dynamical variable.

Each tempering implementation presents its own characteristics and advantages, as recently discussed in details in [14] (see also the Refs. therein). In particular, although the ST has a higher probability than the PT to exchange temperature [14–18], it displays a less frequent tunneling between coexisting phases [14]. Hence, the ST requires large computational time for generating uncorrelated configuration with a slower convergence to the steady equilibrium. On the other hand, for proper estimates (at least at first-order phase transition regimes) the PT needs non-adjacent switch of temperatures, making the procedure a bit more involving – an implementation not necessary for the ST.

Furthermore, for the hard to treat case of strong discontinuous phase transitions, promising extensions for tempering methods have been proposed. In particular, the PT combined with modified ensembles (as multiple Gaussians [19, 20]) comprise the so called generalized

replica exchange approaches [21, 22]. They have been applied with great success to problems like solid-liquid [23] and vapor-liquid transitions [24]. Also, enhancement for the usual ST are possible. Examples are: (a) to consider for it modified distributions [25], leading to very good results for both lattice (e.g., Potts and Ising) and continuum (Lennard-Jones clusters) models; and (b) besides T to assume another dynamical variable, as the external field [26], quite helpful in dealing with crossovers in 2D Ising systems.

Thus, it would be desirable to improve the efficiency of the ST still preserving its positive aspects, notably the procedure simplicity. As a hint to do so, the previous comments indicate that a central point in the ST method is less the probability of a single attempt to exchange temperatures $T_r \rightarrow T_{r+n}$ (with $n = 1$) and more the overall frequency in which the different system phases are visited. Therefore, one should try to optimize the set \mathcal{T}_R as a whole, investigating how the combination of the different transitions would speed up the convergence to the steady state (by a more uniform sampling of the microscopic configurations).

For the ST we then propose here a rather direct protocol to select \mathcal{T}_R by means of a fixed exchange frequency (FEF) prescription. Given R , it consists in determining the T_r 's such that the exchange frequency between any pair of adjacent temperatures is f . From simple preliminary tests we verify if the obtained set leads to an appropriate tunneling between coexisting phases. If this is not the case, another value of f is chosen, a new \mathcal{T}_R is calculated, and the tests repeated. With relatively low computational effort (see next Section), we end up with a very efficient \mathcal{T}_R for the full simulations. Through examples, we furthermore show that this optimal \mathcal{T}_R works well for other values of the considered parameters and not only for the specific values employed in the set derivation. The same \mathcal{T}_R also can be used in the vicinity of the original parameters values as well as for other system sizes. Hence, in many applications \mathcal{T}_R needs to be determined just once. We compare the FEF with other schemes to select the T_r 's. We find that the present is not only superior to more simple recipes (like arithmetic progressions (AP)) but also to more physically oriented selection methods (like the constant entropy (CE) [27, 28]). We finally confirm a somehow expected result (but not fully investigated in the literature) that the exact distribution of temperatures in \mathcal{T}_R becomes less relevant as R increases.

As illustrations, we address three distinct systems, so exploiting a relatively larger variety of first-order phase transitions features. One is the Potts model, an ideal case test. For large q 's, it presents strong discontinuous transitions (the regime we shall focus), whose temperatures are exactly known. The others are the BEG and BL models, likewise interesting not only by displaying more complex phase diagrams than the Potts (e.g., having phases with distinct structural properties), but also for already being extensively analyzed through the PT

and ST approaches [14, 28, 29]. Thus, all them are nice examples to check for the reliability of the proposed protocol.

The work is organized as the following. In Sec. II we review the ST approach and how to characterize first-order phase transitions at low T 's (the context we focus in this contribution). We also discuss in full details the FEF protocol. In Sec. III we analyze the BEG, Bell-Lavis (BL), and Potts lattice models. For the BEG and BL we also compare the FEF results with those for two other schemes (AP and CE) and illustrate the methods performance dependence on the number of replicas R . Lastly, we present final remarks and conclusion in Sec. IV.

II. THE METHOD DETAILS

In general, for systems displaying first-order transitions at low temperatures or with a large jump in the order parameter [30], the distinct coexisting phases are separated by large free-energy barriers, exhibiting trapping and metastable states. Hence, such cases are interesting instances to test the proposed scheme. So, next we first give a brief account of the ST method and discuss an appropriate way to analyze strong first-order phase transitions. Then, we pass to describe a FEF framework for the ST method.

A. The Simulated Tempering (ST)

The ST follows a twofold procedure. First, at a certain T_r (and during some established number of steps), a standard Metropolis prescription evolves a system of Hamiltonian \mathcal{H} throughout the phase space allowed microstates $\{\sigma\}$. Second, an attempt for the change $T_{r'} \rightarrow T_{r''}$ (with $r', r'' = 1, 2, \dots, R$; $\beta_r = 1/(k_B T_r)$; and σ the system state at the attempt time step) is drawn from

$$p_{r' \rightarrow r''} = \min\{1, \exp[(\beta_{r'} - \beta_{r''})\mathcal{H}(\sigma) + (g_{r''} - g_{r'})]\}. \quad (1)$$

This scheme is repeated a number N of times. Also, we consider only adjacent exchanges, i.e., $\Delta r = |r'' - r'| = 1$.

According to Eq. (1), the transition probability $p_{r' \rightarrow r''}$ strongly depends on the temperatures difference. Larger $\beta_{r'} - \beta_{r''}$ leads to lower acceptance probabilities, whereas lower $\beta_{r'} - \beta_{r''}$, although enhancing the exchanges, may not be efficient since the generated configurations at $T_{r''}$ in general will be similar to those at $T_{r'}$. Therefore, conceivably there is a compromise between opposite factors, implying in the existence of a best set \mathcal{T}_R .

Finally, we comment that in some ST implementations, the correct weights $g_r = \beta_r f_r$ (with f_r the free energy) – whose role is to assure an uniform visit to the distinct T 's – are approximated [15, 31]. For our examples, we obtain the g 's exactly by means of the approach in [29, 32]. In short (full details in [14, 29, 32, 33]), suppose a lattice

model composed of K layers of L sites each. The total number of sites (or the volume) is then $V = L \times K$. Also, assume the full Hamiltonian written in terms of these layers as

$$\mathcal{H} = \sum_{k=1}^K \mathcal{H}(S_k, S_{k+1}), \quad (2)$$

where $S_k \equiv (\sigma_{1,k}, \sigma_{2,k}, \dots, \sigma_{L,k})$ denotes the k -th layer state configuration and $S_{K+1} = S_1$ (periodic boundary conditions). The transfer matrix \mathbf{T} is defined in such way that its elements are $\mathbf{T}(S_k, S_{k+1}) = \exp[-\beta \mathcal{H}(S_k, S_{k+1})]$. Thus, in the thermodynamic limit (achieved already at relatively small V 's [29]) $f_r = -\ln[\lambda^{(r)}]/(\beta_r L)$, with

$$\lambda^{(r)} = \frac{\langle \mathbf{T}(S_k, S_{k+1} = S_k) \rangle}{\langle \delta_{S_k, S_{k+1}} \rangle} \Big|_{\beta=\beta_r}. \quad (3)$$

In the above expression, the averages $\langle \dots \rangle$ are directly calculated from usual MC simulations [29].

B. Characterizing the phase transition

For strong first-order phase transitions – our interest here – usual order parameters (such as density and magnetization) and even other thermodynamic quantities like energy, are very well described by expressions in the following generic functional form [34, 35]

$$W \approx (b_1 + \sum_{n=2}^{\mathcal{N}} b_n \exp[-a_n y]) / (1 + \sum_{n=2}^{\mathcal{N}} c_n \exp[-a_n y]). \quad (4)$$

For ξ the control parameter, $y = \xi - \xi^*$ denotes the “distance” to the coexistence point ξ^* and \mathcal{N} is the number of coexisting phases. The c_n 's are constants and the b_n 's are related to $\partial f_n / \partial \xi$, for f_n the free energy of the coexisting phase n [35]. Only the a_n 's are (linear) functions of V . As a remarkable consequence, by considering different system sizes, all curves $W \times \xi$ cross at $\xi = \xi^*$.

Thus, if a numerical approach can properly simulate a given thermodynamic quantity in a phase space region nearby the coexistence point, then simple fittings using Eq. (4) – for just few system sizes L 's – can fully determine the phase transition thermodynamic properties (for many examples and a very detailed discussion about the usage of Eq. (4), see Ref. [35]). We emphasize that for first-order phase transitions at small T 's, the above expression is a rigorous result. In this way, W provides a very reliable test for the method. Indeed, if the simulations lead to order parameters not having the shape in Eq. (4), this is a strong indication of the algorithm inadequacy.

So, assume a fixed L and ξ around the phase transition point ξ^* . We can verify the protocol convergence towards the order parameter steady value as well as the tunneling between the phases as the following. Appropriate sampling of the relevant regions in the phase space

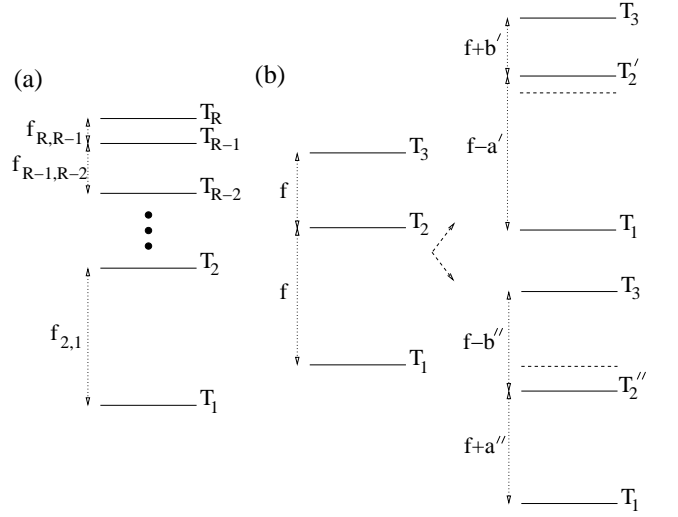


FIG. 1. (a) Given $\mathcal{T}_R = \{T_1, \dots, T_R\}$, successful attempts in changing the system temperature $T_r \rightarrow T_{r+1}$ will give rise to an exchange frequency $f_{r+1,r}$. The FEF protocol requires \mathcal{T}_R to be chosen so that for any r , $f_{r+1,r} = f$. (b) For $R = 3$, small variations in the intermediate temperature T_2 will modify the FEF exchange frequency f as indicated (with $a, b > 0$).

is achieved when the W 's fluctuate mildly around W_0 , with $\bar{W} \approx W_0$ (in our examples averaged over more than 100 simulations runs). On the contrary, trapping in one of the n phases (even for $\xi = \xi^*$) will result in simulated W 's substantially differing from W_0 , in fact closer to the W_n of phase n . Another hint of a good performance is to have $W(L, \xi^*) \approx W_0(L)$ regardless of L . Lastly, an extra checking is to calculate $\partial W / \partial \xi$ and $\chi = (\langle W^2 \rangle - \langle W \rangle^2) V$. Trapping implies in low fluctuations, i.e. $\chi \sim 0$, whereas frequent visit to the distinct regions gives $\chi^* = (\partial W / \partial \xi)|_{\xi^*}$. At the coexistence, $\chi^* \sim V$.

C. Obtaining an efficient set \mathcal{T}_R

As already mentioned, given R , distinct key aspects – specially for the ST [36] – are involved in the T_r 's choice. One example is the actual value of T_R . Indeed, higher T_R 's facilitate the system to escape from the metastable states at T_1 (the temperature of interest). But then, the exchange probability may be too low. Conversely, the frequency of exchanges certainly increases for lower T_R 's, but this time the trapping might not be overcome. Of course, one solution would be to use many replicas, however to the expense of lengthy simulations.

To simplify and improve the determination of \mathcal{T}_R , we propose the following protocol. Once fixed T_1 , we choose $T_1 < T_2 < T_3 < \dots < T_R$ in such a way that the resulting exchange frequencies $f_{r+1,r}$ between any two successive temperatures T_r and T_{r+1} are all equal to some value f (Fig. 1). We define $f_{r+1,r} = N_{r+1,r} / N_{MC}$, with N_{MC} the number of time steps in a Monte Carlo run. Note that

the highest temperature, T_R , is automatically established by the procedure, an advantage in contrast with some other recipes (see below).

The next step is to “probe” the efficiency of the obtained \mathcal{T}_R by means of tests like those described in the end of Sec. II-B. The existence of trapping indicates that T_R is low and f should be decreased, raising T_R . On the opposite, a very high T_R (resulting from a too low f) implies in a very small fraction of exchanges and hence poor averages, so f should be increased. An optimal tuning (respect to the present recipe) will lead to f_{opt} , given rise to a balanced tunneling between the phases and a faster convergence to the steady state. This would accelerate the calculations and improve the estimates accuracy.

Finally, three technical aspects must be pointed out. First, some numerical work is necessary to find f_{opt} . However, such process demands relative short simulations (e.g., it is not necessary to evolve the system until full convergence). Thus, the search for the corresponding optimal \mathcal{T}_R is not computationally time consuming.

Second, usually one shall study phase transitions in a region, instead only at one point Λ , of the parameters space. From the exploratory numerics we have performed (representative examples in Sec. III), we found that once an optimal set of temperatures is determined for a specific Λ , in a not too small vicinity around it the same set also yields rapid and good results. So, in exploring sectors of the parameters space one needs to find only few optimal \mathcal{T}_R 's. In particular, \mathcal{T}_R does not significantly change for reasonable different system sizes L . Therefore, the procedure can be helpful for finite scale size analysis [34].

Third, T_R for f_{opt} is a value which at once allows enough temperatures exchanges, yet resulting in proper tunneling between the phases. Thus, an eventual further improvement of \mathcal{T}_R should not drastically change T_R , just modifying the intermediate temperatures T_2, \dots, T_{R-1} . From our construction, at f_{opt} the combined exchange frequency from T_1 to T_R is roughly proportional to $F_{R,1} \sim (f_{opt})^{R-1}$. Let us consider Fig. 1 (b) with $R = 3$. Increasing (decreasing) T_2 , with $T_2 \rightarrow T_2'$ ($T_2 \rightarrow T_2''$), the overall transition frequency $1 \rightarrow 3$ ($F_{3,1}^{(\Delta)}$) reads: $F_{3,1}^{(\Delta)} \sim f_{opt}^2 + (b' - a')f_{opt} - b'a' (f_{opt}^2 + (a'' - b'')f_{opt} - b''a'')$. Although we have not been able to derive expressions for the a 's and b 's, from exhaustive numerics we never found a 's and b 's making $F_{1,3}^{(\Delta)}$ considerably larger than $F_{1,3}$. So, extra variations of the T_r 's around the values in the optimal \mathcal{T}_R makes the procedure much more cumbersome and does not seem importantly to improve the method.

III. RESULTS

Here we apply the FEF approach to three lattice models, BEG, BL, and Potts, also comparing some results with those for the ST using other schemes to select \mathcal{T}_R . So, we need first to brief discuss few distinct methods to obtain the T_r 's.

Some proposals are rather simple, usually not taking explicit into account the physical aspect of the system (but refers to [37, 38] for the particular case of constant specific heats). The exception being usually the numerical procedure to set the final temperature T_R [39]. Along this line, one example is to assume (given R , T_1 and T_R) the intermediate temperatures forming an arithmetic progression (AP) [40] (see also [14]).

A more thermodynamic-oriented method is the constant entropy (CE) protocol, proposed in [27, 41] (and extended in [28] for distinct lattice-gas models). It consists of choosing intermediate T_r values so to lead to a same fixed difference of entropy between successive temperatures (but again, somehow T_R must be first determined). Specifically, if at T_1 and T_R the system entropy per volume is, respectively, s_1 and s_R , we set T_r such that $s_r = s_1 + (r - 1)(s_R - s_1)/(R - 1)$. Once the transfer matrix method of Sec. II-A gives the free energy, the evaluation of entropies for the CE protocol follows from $s_r = (u_r - f_r)/T_r$, where $u = \langle \mathcal{H} \rangle$.

Thus, an immediate advantage of FEF with respect to both AS and CE is that it directly provides an optimal T_R necessary for the system to circumvent the entropic barriers. We also observe that close to the phase transition, where a small change of the control parameter results in a great variation of s , the FEF and the CE yield more clustered T_r 's. Because quantities like u and s undergo pronounced changes around the phase transition, a clustered \mathcal{T}_R is in general more efficient. So, in advance one should expect CE and FEF better than AS.

A. The models

1. BEG

The BEG [42] is a generalization of the Ising model, where the spin variable presents three values $\sigma_i = 0, \pm 1$. In a fluid language, it corresponds to a lattice-gas model with distinct species (\pm) and vacancies (0). The Hamiltonian also presents an extra interaction term, proportional to $\sigma_i^2 \sigma_j^2$, reading

$$\mathcal{H} = - \sum_{\langle i,j \rangle} (J \sigma_i \sigma_j + K \sigma_i^2 \sigma_j^2) - \mu \sum_i \sigma_i^2, \quad (5)$$

for J and K interaction energies and μ the chemical potential. Its phase diagram is relatively complex, displaying phases with distinct structural properties. For the K 's we consider here and in the regime of low temperatures, a first-order transition separates liquid and gas phases for high and low chemical potentials, respectively. The order parameter is the particle density $\rho = \langle \sigma_i^2 \rangle$. At the steady state the system presents two liquid phases (with densities close to 1) coexisting with one gas phase (of $\rho \approx 0$). Since they have equal weights, $W_0 = \rho_0 = (1 \times 0 + 2 \times 1)/(1 + 2) = 2/3$. For $T = 0$, the liquid-gas phase coexistence emerges at $\mu^* = -z(K + 1)/2$, with

z the coordination number. By increasing T , an order-disorder phase transition takes place, being continuous or discontinuous depending on how high is T .

The transfer matrix, used to evaluate the weights for the ST method and the entropy, is given by

$$\mathbf{T}(S_k, S_{k+1} = S_k) = \exp \left[\beta \sum_{i=1}^L \left(J \sigma_{i+1,k} \sigma_{i,k} + (J + \mu + K(1 + \sigma_{i+1,k}^2)) \sigma_{i,k}^2 \right) \right]. \quad (6)$$

2. Bell-Lavis (BL)

The BL is the simplest orientational model reproducing water-like features, including thermodynamics, dynamics and anomalous solubility [43–45]. It is defined on a triangular lattice and described by two kind of variables. σ_i determines if the site i is either empty (0) or occupied (1) by a molecule. On the other hand, τ_i^{ij} indicates the possibility of hydrogen bonding formation between adjacent molecules. Each molecule has six arms (in angles of 120°), such that three of them are inert, while the other three are the bonding arms. If at a site i there is a molecule pointing its bonding arm towards the site j , then $\tau_i^{ij} = 1$, otherwise $\tau_i^{ij} = 0$. For ϵ_{vdw} and ϵ_{hb} the van der Waals and hydrogen bonds interaction energies, the BL model is defined by the following Hamiltonian

$$\mathcal{H} = - \sum_{\langle i,j \rangle} \sigma_i \sigma_j (\epsilon_{hb} \tau_i^{ij} \tau_j^{ji} + \epsilon_{vdw}) - \mu \sum_i \sigma_i. \quad (7)$$

For $\zeta = \epsilon_{vdw}/\epsilon_{hb} > 1/3$ (the case we discuss here) the system has three stable phases, gas, low-density-liquid (LDL) and high-density-liquid (HDL) [43, 46], emerging as one increases μ . In the gas phase, molecules are scarce and unstructured ($\rho \approx 0$), whereas in the LDL phase (absent in the BEG model), the molecules are organized in a honeycomb network, with a density of $\rho = 2/3$. In the HDL phase, the lattice is nearly fully filled with $\rho = 1$. Also in contrast with the liquid phase for the BEG model, the HDL phase is highly degenerated. At $T = 0$, gas-LDL and LDL-HDL transitions are first-order and occur at $\mu^* = -3(1 + \zeta)/2$ and $\mu^* = -6\zeta$, respectively. For $T \neq 0$, the gas-LDL remains first-order, whereas LDL-HDL becomes second-order [43]. For $\zeta = 0.1$, the second- and first-order lines meet at a tricritical point. The order parameter for the gas-LDL is the density, hence $W = \rho$. At the phase coexistence, $\rho_0 = 1/2$ (understood from the fact that the LDL phase has degeneracy 3 and since their weights become equal at the phase coexistence, the value $\rho_0 = (1 \times 0 + 3 \times 2/3)/(1 + 3) = 1/2$ follows).

The transfer matrix reads

$$\mathbf{T}(S_k, S_{k+1} = S_k) = \exp \left[\beta \sum_{i=1}^L \left(\sigma_{i,k} (\sigma_{i,k} + 2\sigma_{i+1,k}) \times (\epsilon_{vdw} + \epsilon_{hb} \tau_{i,k} \tau_{i+1,k} + \mu) \right) \right]. \quad (8)$$

3. Potts model

The Potts [47] is a simple spin lattice model for which the variable σ_i (defined on the site i) takes the integer values $0, 1, \dots, q-1$. Adjacent sites i' and i'' have a non-null interaction energy of $-J$ whenever $\sigma_{i'} = \sigma_{i''}$. The problem full Hamiltonian reads

$$\mathcal{H} = -J \sum_{\langle i,j \rangle} \delta_{\sigma_i, \sigma_j}. \quad (9)$$

For small temperatures the system is ordered, becoming disordered as T increases. The transition point is exactly given by $T_c = 1/\ln[1 + \sqrt{q}]$. In 2D, for $q \leq 4$ the phase transition is of second-order and discontinuous if $q \geq 5$. A proper order parameter $W = \phi$ is

$$\phi = \frac{q(V_{max}/V) - 1}{q - 1}, \quad (10)$$

where V_{max} is the volume occupied by the spins of the state s of largest population and $V = L^2$.

For the Potts, the transfer matrix yields

$$\mathbf{T}(S_k, S_{k+1} = S_k) = \exp \left[\beta J \sum_{i=1}^L \left(1 + \delta_{\sigma_{i+1,k} \sigma_{i,k}} \right) \right]. \quad (11)$$

B. Simulations

For the numerics we consider regular lattices with periodic boundary conditions, also setting the Boltzmann constant k equal to 1. For the BEG and Potts we assume a square and for the BL a triangular lattice of volume $V = L \times N$. The parameters used are: $T_1 = 0.5000$, $K/J = 3$, $J = 1$ (BEG), $T_1 = 0.1000$, $\zeta = 0.1$, $\epsilon_{hb} = 1$ (BL), and $q = 20$, $T_1 = 1/\ln[1 + \sqrt{20}] = 0.5883\dots$, $J = 1$ (Potts). Moreover, unless otherwise explicit mentioned $L = N = 20$, $L = N = 18$ and $L = N = 18$ for, respectively, the BEG, BL and Potts models. In all cases we are in the low temperature regime and for BEG and BL strong discontinuous transitions (with coexisting phases separated by large free energy barriers) result from a chemical potential μ_0 close to its $T = 0$ value, so that $\mu_0 = -8.0000(1)$ at $T_1 = 0.5000$ (BEG) and $\mu_0 = -1.6500(1)$ at $T_1 = 0.1000$ (BL). Finally, we recall that for larger T 's, obviously the phase coexistence takes place for distinct values of the chemical potentials (e.g., for the BL and $T = 0.25$, the gas-LDL phase transitions is at $\mu = -1.6528(1)$). In those cases the proposed protocol also works better than other procedures to choose the replicas temperatures (as we have explicit verified). But since then the entropic barriers are lower, the present very strong first-order phase transition is a more interesting context for our comparative analysis.

f	5×10^{-2}	1×10^{-2}	6×10^{-4}	(f_{opt})	10^{-5}
T_1	0.50	0.50	0.50	0.50	0.50
T_2	1.35	1.45	1.60	1.82	1.82
T_3	1.70	1.88	2.05	2.33	2.33

TABLE I. For the BEG model, temperature sets $\mathcal{T}_{R=3}$ for distinct frequencies f .

f	1.1×10^{-1}	5×10^{-2}	2×10^{-2}	(f_{opt})	10^{-4}
T_1	0.50	0.50	0.50	0.50	0.50
T_2	1.25	1.35	1.40	1.45	1.45
T_3	1.55	1.70	1.80	1.88	1.88
T_4	1.78	1.95	2.04	3.20	3.20

TABLE II. The same as in Table I, but for $R = 4$.

1. Results using FEF for the BEG and BL models

For the BEG model, in Tables I and II we show for $R = 3$ and $R = 4$ some sets \mathcal{T}_R obtained with the FEF protocol.

To determine which set \mathcal{T}_R is the best one, in Fig. 2 we compare for the BEG model and $R = 3$ the density evolution towards the steady value $\rho_0 = 2/3$ (we start from a non-typical initial configuration, a lattice totally filled of particles). For larger f 's (e.g., f_1 , f_2 and f_3), despite more frequent temperature exchanges, the system gets trapped in the initial configuration as a consequence of a too low T_3 . On the other hand, for much lowers f 's (as f_6), the resulting T_3 's become high enough to cross the entropic barrier, but then exchanges hardly take place. Hence, there is an optimal intermediate value, f_{opt} , yielding the best convergence to the correct ρ_0 .

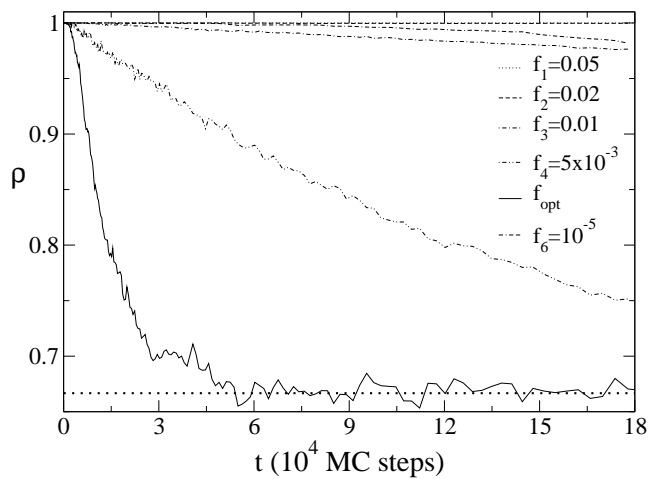


FIG. 2. For the BEG model at the phase coexistence (see main text), ρ simulated with the ST algorithm for the $\mathcal{T}_{R=3}$'s obtained from distinct f 's. The best convergence toward the steady value $\rho_0 = 2/3$ is obtained for $f_{opt} = 6 \times 10^{-4}$.

time scale in Fig. 2, i.e., of 10^4 MC steps. Note in the graph that for f_{opt} , the very fast decay of ρ to its correct value is already evident for small values of t . Therefore, even simulations for times around 10^3 MC would be able to determine f_{opt} . However, the apparently longer than necessary simulation in Fig. 2 has a practical reason. As discussed in [14], specially for the ST method, the computation time \bar{t} need to estimate thermodynamical quantities generally must be longer (at least one order of magnitude) than τ . Here, τ is the typical time to overcome the transients and to reach the steady state (e.g., in Fig. 2, $\tau \approx (3-7) \times 10^4$). In fact, because the many temperatures changes during the whole simulation, the ST requires a proper \bar{t} to ensure enough sampling at the desired T_1 . This point, directly related to tunneling between the phases and exchange rates between the T_r 's, becomes even more relevant at low T 's. Thus, Fig. 2 is also helpful to give an idea about \bar{t} . For instance, for the BEG model, we have $\bar{t} = 3 \times 10^5$ MC steps.

Using the above \bar{t} to make the averages $\langle \rho \rangle$ for the simulated ρ , in Fig. 3 we plot for the BEG model and $R = 3$ and $R = 4$, the percentile difference from $\rho_0 = 2/3$, $\Delta = |2/3 - \langle \rho \rangle| / (2/3) \times 100\%$, as function of $f(\%)$. As it should be, Δ has a minimum for $f = f_{opt}$. We also see that f_{opt} is greater for $R = 4$. This is a direct consequence of the T_R 's to be essentially the same when $f = f_{opt}$ (compare Tables I and II). So, $T_{r+1} - T_r$ is smaller for $R = 4$, yielding a higher f_{opt} . At the optimal condition, $\langle \rho \rangle$ is equal to 0.665(2) and 0.666(1) for $R = 3$ and $R = 4$, respectively.

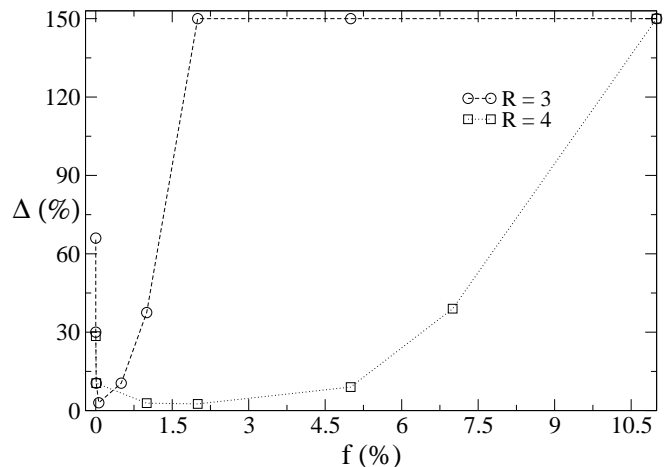


FIG. 3. $\Delta = |2/3 - \langle \rho \rangle| / (2/3) \times 100\%$ as function of $f(\%)$. Δ is a minimum, of 3% and 2.5%, respectively for $R = 3$ and $R = 4$, when $f = f_{opt}$.

Similar analysis have been done for the BL model. In Tables III ($R = 3$) and IV ($R = 4$) we illustrate the results showing few values of f and the associated \mathcal{T}_R 's. From plots like those in Figs. 2 and 3 (not shown here) we have determined the f_{opt} 's as indicated in the tables. Furthermore, for f_{opt} we have estimate that $\bar{t} = 5 \times 10^6$ MC steps. This longer time necessary for the averages

reflects a higher complexity of the BL model, hence more difficult to simulate than the BEG. At the optimal condition, $\langle \rho \rangle = 0.508(5)$ ($R = 3$) and $\langle \rho \rangle = 0.500(4)$ ($R = 4$).

f	2.5×10^{-2}	3×10^{-3}	2×10^{-4}	(f_{opt})	10^{-5}
T_1	0.10	0.10	0.10	0.10	0.10
T_2	0.25	0.28	0.32	0.35	0.35
T_3	0.33	0.38	0.43	0.48	0.48

TABLE III. For the BL model, temperature sets $\mathcal{T}_{R=3}$ for distinct frequencies f .

f	1.5×10^{-1}	7×10^{-2}	1×10^{-2}	(f_{opt})	10^{-5}
T_1	0.10	0.10	0.100	0.10	0.10
T_2	0.20	0.23	0.27	0.29	0.29
T_3	0.25	0.30	0.34	0.39	0.39
T_4	0.29	0.39	0.43	0.50	0.50

TABLE IV. The same as in Table III, but for $R = 4$.

Another important factor to guarantee proper estimates for the thermodynamic quantities is to assure a frequent tunneling between the phases *after* the system to reach the steady state. By plotting ρ for times much larger than \bar{t} , we can further check when this condition is indeed fulfilled for the difference choices of f , Tables I–IV. The simulations are shown in Figs. 4 and Fig. 5, $R = 3$ and $R = 4$, with the left (right) panels displaying the BEG (BL) model. For the largest f 's, (case (a) in both figures) the sets \mathcal{T}_R are rather inefficient and the system stays trapped into one phase. For the f 's in (b) and (d), the density substantially fluctuates about its true equilibrium value ρ_0 . It is exactly for f_{opt} that ρ oscillates much closer to ρ_0 (case (c)), thus leading to the best estimates. As one should expect, overall the better results are those for a larger R , compare Figs. 4 and 5. This is a consequence of a more balanced sampling due to a larger number of replicas, but then requiring greater computation efforts.

Lastly, to verify that at the transition condition (of first-order) in fact the system is properly visiting the co-existing phases, we perform a final important test. After the convergence to the steady state (using $R = 3$ and the optimal set \mathcal{T}_3), we calculate the probability distribution for ρ at the temperature of interest T_1 , assuming different system sizes L . For each L , by properly setting $\mu = \mu_L$ we have the results for the BEG and BL models, respectively, shown in Figs. 6 and 7. In all cases, we see that the probability distributions P_ρ display well defined bimodal shapes, with the peaks at the ρ values of the individual phases. This clearly indicates a first-order phase transition. Moreover, from simple scaling arguments [30] (typically used to locate the coexistence points, see, e.g., [10]), the chemical potential values μ_L should vary linearly with the inverse of the volume (i.e., $\mu_L - \mu_0 \sim 1/L^2$) and give the correct μ_0 in the thermodynamic limit. This is indeed observed in Figs. 6 (b) and 7

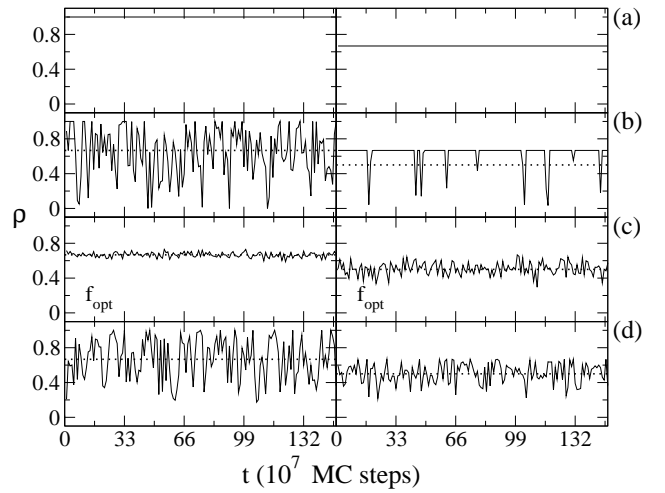


FIG. 4. For $R = 3$, ρ versus the simulation time for t much larger than \bar{t} . The results are for the BEG (left panel) and BL (right panel) models, where (a), (b), (c), and (d) represent the four sets \mathcal{T}_R in the same order presented in Tables I (BEG) and III (BL).

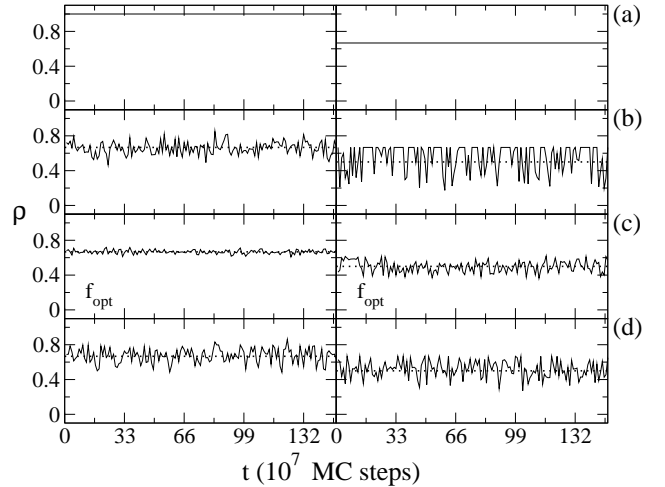


FIG. 5. The same as in Fig. 4, but for $R = 4$. (a), (b), (c), and (d) are for the sets in Tables II (BEG) and IV (BL).

(b), whose extrapolated μ for $1/L^2 \rightarrow 0$ agrees very well with the analysis using the function W in the end of Sec. III-B-2.

An interesting aspect, which can be analyzed from the probability distribution plots, is how the combined distinct phases ρ 's, at the coexistence, lead to the system steady state density ρ_0 . Let us consider the BEG model as an example. As already discussed in Sec. III-A-1, for the BEG $\rho_0 \approx 2/3$ since exactly at transition we have two phases with $\rho = 1$ and one with $\rho \approx 0$, all contributing with a same weight. This is indeed verified in Fig. 2. In Fig. 6 (a), for different μ_L 's and L 's, the P_ρ is strongly concentrated in $\rho = 0$ and $\rho = 1$, as it should be. However, the peaks heights are not in the proportion 1:2. This is so because for the μ 's and L 's considered in

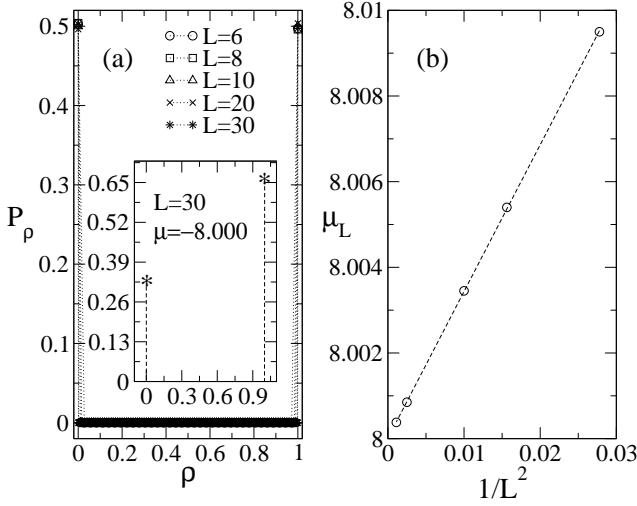


FIG. 6. For the BEG model, (a) the probability distribution histogram P_ρ of the order parameter ρ at the coexistence for distinct system sizes L . The different distributions – each calculated at a given chemical potential value μ_L – are clearly bimodal (with the gas phase having $\rho \approx 0$ and the two liquid phases having $\rho = 1$). In the inset, P_ρ for $\mu = -8.000$ and $L = 30$. In (b), the μ_L 's in (a) vs. the inverse of the volume $1/L^2$. Extrapolating to the thermodynamic limit (i.e., infinite volume), one gets $\mu = -8.00000(5)$, in very good agreement with $\mu_0 = -8$ (main text).

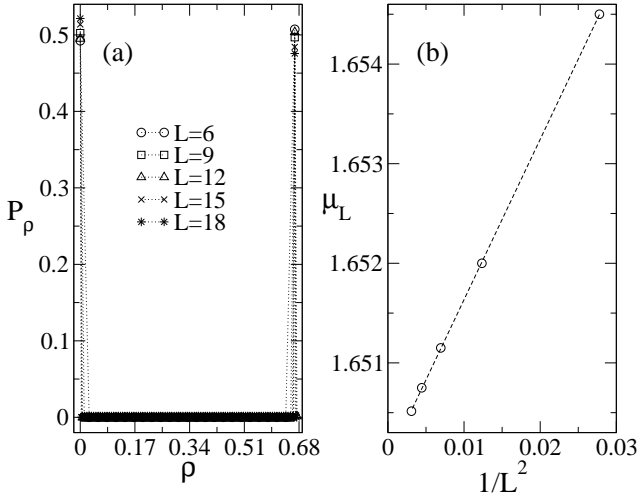


FIG. 7. The same as in Fig. 6, but for the BL model. Here, an extrapolation from (b) leads to $\mu = -1.65000(5)$, in agreement with $\mu_0 = -1.65$.

the graphs, we are not still at the thermodynamic limit, when the equal probability for the phases does hold. In contrast, for $\mu = -8.000$, P_ρ in the inset of Fig. 6 (a) exhibits the expected 1:2 ratio. Although not explicit shown, this behavior is also the case for the BL model in Fig. 7.

Finally, we observe that as discussed in details in Refs. [14, 29] for the BEG and in Refs. [29, 35] for the BL, these systems also go through strong first order phase

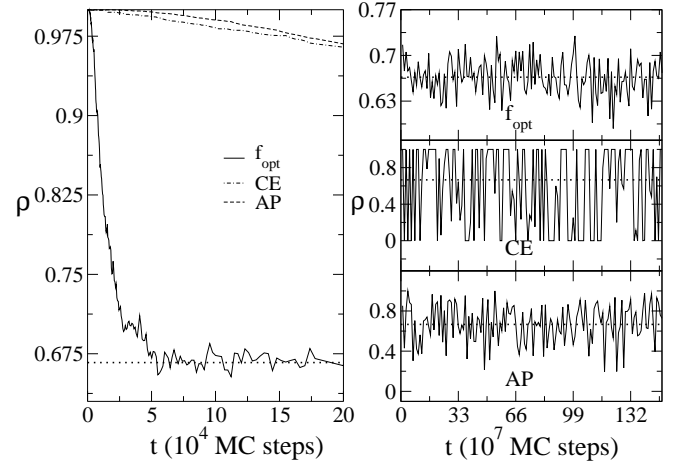


FIG. 8. For the BEG model, simulations from the ST method with $R = 3$ replicas and different schemes to determine \mathcal{T}_R . Left panel: ρ during the transient time (towards the steady state). Right panel: ρ versus time (in MC steps) – already at the steady state – showing how each temperature set makes the system to tunnel between the coexisting phases (observe the different ρ scales in each plot). The dotted lines indicate the correct $\rho_0 = 2/3$. The temperature set for AP follows directly (since T_1 and $T_{R=3}$ are given) and the intermediate temperature for the CE is $T_2 = 1.88$. Also, $\langle \rho \rangle_{CE} = 0.61(5)$ and $\langle \rho \rangle_{AP} = 0.67(2)$.

transitions for temperatures three times as higher as the ones used here. Nevertheless, in such cases the choice of \mathcal{T}_R is not so critical as for the T 's in the present work (see, e.g., the discussion in [28]).

2. Comparison with other \mathcal{T}_R schemes for the BEG and BL

Now, we compare the FEF with some other available protocols to set \mathcal{T}_R , namely, AP and CE. To facilitate their implementation (recall that AP and CE do not have a specific rule to determine the maximum temperature), we use for them the same value of T_R found from the FEF in the optimal condition.

For the BEG model (for the BL the results are similar, thus not shown here) we analyze the density time evolution toward the steady state and the tunneling between coexisting phases in Figs. 8 ($R = 3$) and 9 ($R = 4$). It is clear that the FEF recipe provides the fastest convergence towards ρ_0 . In addition, the tunneling between the phases is also substantially more frequent than for AP and CE.

Although the FEF is systematically better than AP and CE, the difference is less pronounced for $R = 4$. This should be expected since for a larger number of replicas, provided T_R is properly chosen, the exact values of the intermediate T_r 's do not play a so critical role. To further illustrate this fact, we repeat the simulations of Figs. 8 and 9, but now using $R = 6$. This is displayed in Fig. 10 for BEG and BL models, where it is

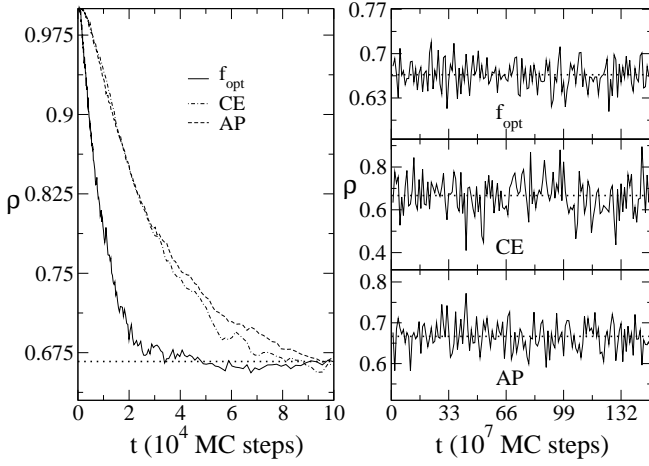


FIG. 9. The same as in Fig. 8, but for $R = 4$. For the CE scheme, the intermediate temperatures are $T_2 = 1.75$ and $T_3 = 1.95$. Also, $\langle \rho \rangle_{CE} = 0.661(6)$ and $\langle \rho \rangle_{AP} = 0.666(3)$.

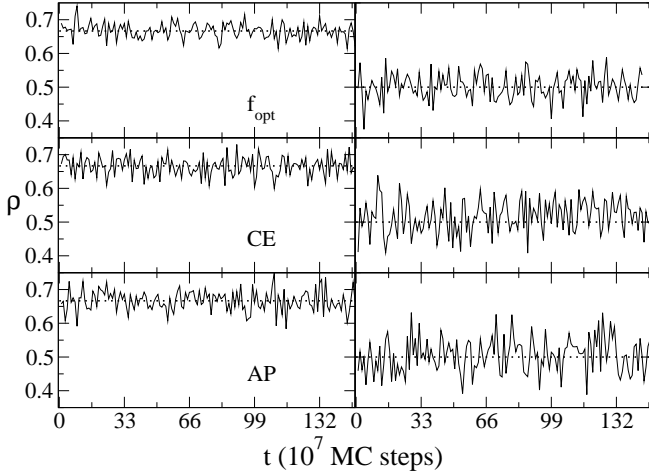


FIG. 10. ρ versus t for the BEG and BL, left and right panels, at phase coexistence and distinct \mathcal{T}_R schemes, with $R = 6$. In all cases the extreme temperatures are $T_1 = 0.5$, $T_6 = 2.06$ (BEG) and $T_1 = 0.1$, $T_6 = 0.43$ (BL). For the f_{opt} and CE recipes, the intermediate temperatures are, respectively: $\{1.25, 1.55, 1.78, 1.95\}$ and $\{1.61, 1.82, 1.94, 2.00\}$ (BEG); and $\{0.23, 0.30, 0.32, 0.39\}$ and $\{0.31, 0.36, 0.40, 0.41\}$ (BL).

shown the tunneling frequency after the transient. Visually, the distinct schemes seems to give the same results (but note a smaller statistical uncertainty, fluctuation, for the FEF). We get $\langle \rho \rangle$ from the f_{opt} , CE and AP, respectively equal to, 0.667(2), 0.666(2), and 0.666(2) for the BEG and 0.501(3), 0.52(1), and 0.51(1) for the BL. These values should be compared to $\rho_0 = 2/3 = 0.666\dots$ for the BEG and $\rho_0 = 0.5$ for the BL. Actually, the FEF still gives a little more accurate estimates, specially for BL.

Although one of the nice features of the ‘combo’ approach here – to combine Eq. (4) with the ST using an optimal choice for \mathcal{T}_R – is to be able to obtain the

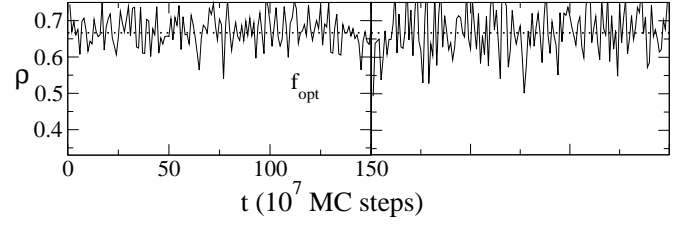


FIG. 11. ρ versus t for the BEG model at phase coexistence for the $R = 6$ optimal temperature set and two large L values.

thermodynamic limit for discontinuous transitions from considerably small systems [34, 35] (see next), the same scheme in principle does also work well for large L ’s. For instance, for the BEG model, we consider in Fig. 11 the previous optimal set obtained for $R = 6$ replicas (Fig. 10), but now simulating sizes of $L = 30$ and $L = 40$. As it can be seen, the proper tunneling between coexisting phases confirms that a same optimal \mathcal{T}_R can be used for distinct big L ’s.

As already stated, some initial numerical work necessary to determine the optimal \mathcal{T}_R (for a specific point Γ of the parameters space) pays off not only because then the full simulations are faster and more reliable, but also because this same set could be used for other points in the vicinity of Γ . To exemplify this, we consider the ST method with $R = 3$ and use the optimal $\mathcal{T}_{R=3}$ in Tables I (BEG) and III (BL) – determined for $\mu = \mu_0$ and L as in Sec. III B 1. Then, we calculate ρ for distinct values of the chemical potential μ and system size L . The results are shown as symbols in Fig. 12. In all the simulations we have obtained fast and good convergence to the steady state and frequent tunneling between phases exactly as in our previous analysis. The continuous curves are fits given by the general expression W , Eq. (4), which is the correct shape of the order parameter ρ in a first-order phase transition at low temperatures [34]. The very good matching between the simulated points and the smooth curves W illustrate that indeed ρ versus μ for different L ’s is well described by our approach from just one \mathcal{T}_R . Furthermore, the crossings take place at $\mu = -8.000(1)$ (BEG) and $\mu = -1.6500(1)$ (BL), as it should be (see Sec. III-B-1).

3. The FEF method for the Potts model

f	4×10^{-1}	1×10^{-1}	5×10^{-2}	(f_{opt})	2×10^{-2}
T_1	0.5885	0.5885	0.5885	0.5885	0.5885
T_2	0.5945	0.6030	0.6054	0.6100	0.6100
T_3	0.5972	0.6245	0.6260	0.6300	0.6300

TABLE V. For the Potts model, temperature sets $\mathcal{T}_{R=3}$ for distinct frequencies f .

The Potts is an interesting (and also challenging) sys-

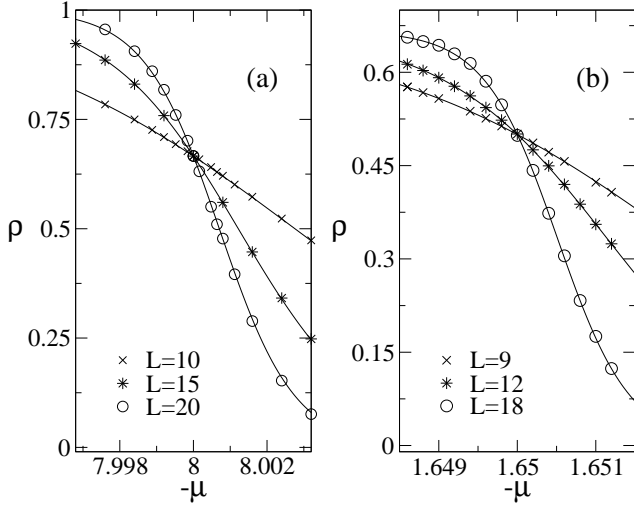


FIG. 12. ρ versus the chemical potential μ (for distinct L 's) for the (a) BEG and (b) BL models. The simulations (symbols) are performed with the ST method, for $R = 3$ and the set \mathcal{T}_R corresponding to f_{opt} in Tables I and III. The continuous lines are fits using the general functional form W for ρ (where only four simulated points are necessary to determine the coefficients a , b and c in Eq. (4)).

tem to analyze given the existence of strong first-order phase transitions for high values of its parameter q . Hence, the model is frequently used as a benchmark to test different numerical algorithms (see, for instance, Refs. [20, 22, 25, 35]). So, next we present some of our previous discussions regarding the efficiency of the FEF protocol considering the Potts with $q = 20$ (therefore, already a large value in the above mentioned respect).

For $R = 3$, in Table V we show the temperatures values for distinct choices of f . Due to the strong transition presented by the problem for $q = 20$, from the simulations determining the f 's we estimate $\bar{t} = 10^7$ MC steps, thus higher than, e.g., $\bar{t} \sim 10^5$ obtained for the BEG model. In Fig. 13 we plot the order parameter ϕ , Eq. (10), and the energy $u = \langle \mathcal{H} \rangle$ as function of t for distinct f 's. Averages are evaluated each $\bar{t} = 10^7$ MC steps. Dotted lines are steady values obtained from a very precise approach (and more complex than the present one) developed in [35], which combines cluster algorithms, the PT method and semi-analytic protocols to enhance tunneling between the different coexisting phases.

The behavior of both ϕ and u in Fig. 13 is in agreement with that observed for the BEG and BL order parameters. There is an optimal value of f , f_{opt} , allowing substantially more frequent tunnelling between phases and thus much better statistics to calculate relevant thermodynamic quantities. On the other hand, “fortuitous” choices for \mathcal{T}_R (arbitrary f 's) yield poor results and an eventual impression that the usual ST approach could not handle strong first order phase transitions.

Lastly, we perform an analysis similar to that shown in Fig. 12 for the BEG and BL models. For Fig. 14 we:

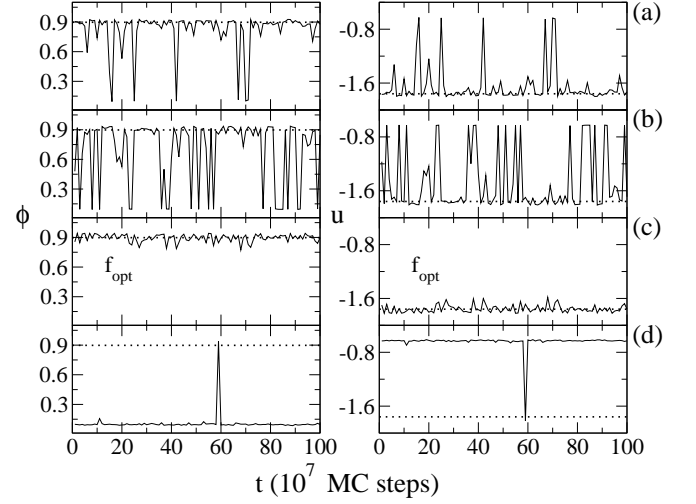


FIG. 13. For $R = 3$, ϕ and u versus the simulation time t for the Potts model. The results in (a), (b), (c), and (d) represent the four sets of $\mathcal{T}_{R=3}$ displayed in Table V.

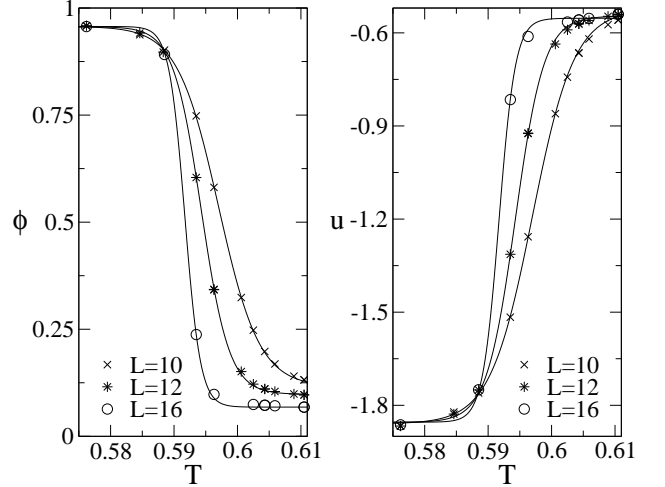


FIG. 14. For the Potts model and $R = 3$, ϕ and u versus the temperature T for three values of L . The simulations (symbols) are performed with the set \mathcal{T}_R corresponding to f_{opt} in Table V. The continuous lines are fits using the general functional form W and only four simulated points.

consider distinct T 's around the $q = 20$ Potts transition temperature, use the same f_{opt} in Table V – found for $T = 0.5883 \dots$ – to form sets $\mathcal{T}_R = 3$ (with $T_1 = T$), and calculate ϕ and u as function of such T 's. Again we see that the present method provides very precise values (as it can be confirmed, e.g., by comparing with Ref. [35]) for both order parameter and energy (well described by Eq. (4)). However, we should mention that in [35] it was necessary to combine cluster algorithms and the PT (with non-adjacent exchanges and larger number of replicas) for the system to properly cross the coexisting phases. Hence, the results here have been obtained with much less computational efforts.

It is also worth contrasting ours with some studies combining generalized ensembles with the PT [21] and ST [25] algorithms. In these works, the methods efficiency for the Potts model are indeed very good, nevertheless comparable with the ST-FEF in terms of numerical precision and computational time. Also, in Refs. [21, 25] $q = 8$, hence a weaker transition than here. However, the simulations are done for systems up to $L = 64$, so much larger than the present ones ($L = 18$). But they use $R = 30$ replicas. In Figs. 13 and 14, we have been able to obtain proper convergence just with $R = 3$ and small systems (the latter in part thanks to the use of our semi-analytic fitting, Eq. (4)).

IV. FINAL REMARKS AND CONCLUSION

In this contribution we have proposed a simple method to determine the set of T_r 's for the ST algorithm. For a given number of replicas R , adjacent T_r 's are chosen in such a way that changes of temperature (from T_r to T_{r+1} , for any $r = 1, 2, \dots, R-1$) occur with a fixed frequency f . Then, from simulations demanding a relative small number of time steps we test, e.g., the decay toward the steady regime and the tunneling rate between distinct coexisting phases. Such tests can benchmark the efficiency of \mathcal{T}_R resulting from this f . Repeating the procedure, it is possible to find an optimal f_{opt} leading to a best \mathcal{T}_R (including a proper T_R). Note that for some other schemes, there is no specific rules to determine the extreme temperature necessary for the system to cross the entropic barriers.

The searching for f_{opt} demands some preliminary numerics, nevertheless twofold compensated. First, the full simulations – for the final estimation of the thermodynamical quantities – will converge faster and with greater accuracy. Second, the same optimal \mathcal{T}_R can be used to simulate the system for other parameters values, around the original Γ used to determine f_{opt} .

The reliability and precision of the FEF scheme have been analyzed in the extreme situation of systems presenting first-order phase transitions at low T 's. In all examples we have obtained very good thermodynamic estimates (even for $R = 3$) without the necessity of long simulations. In fact, one of the advantages of using the FEF to select \mathcal{T}_R is that once at the optimum case, the results are already very good for R small, hence facilitating the numerical implementation. Furthermore, comparison with other temperature schemes, AP and CE, have been undertaken. The FEF has been found to be always superior to the others, specially for small R 's.

To conclude, we shall comment on the following. First, in the last few years distinct protocols have been proposed for dealing with the difficult situation of first-order transitions at low T 's. In particular, Ref. [19] shows how to increase visits to regions of high free-energies (hence with very low probability to be accessed) considering additional multiple Gaussian weights for the ensembles de-

scribing the system. Moreover, a combination with the parallel tempering is used for restoring ergodicity. In Ref. [25] it is devised an adaptive (“on the flight”) approach for the ST weights, whose evaluations follow a modified distribution [48]. In fact, using the ST with independent modified-weight runs, the tunneling between the phases is strongly facilitated.

Although certainly the above methods are of very broad usage and important contributions to handle such hard problem, our proposal somehow strikes in a different direction. Actually, not only the free energy weights are evaluated directly from standard MC simulations (so, without no effective resampling procedures, which eventually could depend on systems particularities), but also adequate “probing” of the phase space distinct regions are achieved solely from the tempering. As shown, the crucial point is to determine a good temperature set, possible through relative inexpensive simulations. Thus, our approach is easier to implement and can be faced as a generic algorithm, not requiring too much details about the specific system. The mentioned methods are very efficient, but may demand elaborate implementations focusing the specific case at hands (e.g., properly tuning dynamic dependent parameters).

Second, although we have used an optimized protocol to determine \mathcal{T}_R for a tempering method, applying it to first-order transitions (where the specific T_r 's may be crucial), we believe the main ideas here can also be useful for second-order phase transitions. Indeed, in second-order phase transitions the trapping in metastable states is not generally present. However, at the criticality the system is strongly affected by a slow time decay of correlation functions (critical slowing down) [14]. In such case, an optimal \mathcal{T}_R might provide a faster decay of correlations, thus allowing a more precise evaluation of the system properties. In fact, a practical way to achieve so would be to find f_{opt} which minimizes the relaxation time τ of a given relevant correlation function.

Third, in the so called parallel tempering (PT), usually exchanges of temperature are not restricted to adjacent replicas (T_r and T_{r+1}), hence the exact set \mathcal{T}_R is not so crucial (but see [49]). Nevertheless, a simpler algorithm using only adjacent exchanges eventually would require a more appropriate choice for \mathcal{T}_R , which could then be determined by the FEF.

The above two possible applications for our method are presently being implemented and will be reported in the due course.

V. ACKNOWLEDGMENT

We acknowledge research grants from CNPq and computational facilities provided by CT-Infra-Finep and CNPq-Edital Universal.

REFERENCES

-
- [1] K. Binder, W. Kob, *Glassy Materials and Disordered Solids: An Introduction to their Statistical Mechanics*, World Scientific, Singapore, 2005.
- [2] J. Skolnick, A. Kolinski, *Comput. Sci. Eng.* 3 (2001) 40.
- [3] V. S. Pande, A. Y. Grosberg, T. Tanaka, *Rev. Mod. Phys.* 72 (2000) 259.
- [4] M. Allen, D. J. Tildesley, *Computer Simulation of Liquids*, Oxford University Press, Oxford, 1987.
- [5] D. Frenkel, B. Smith, *Understanding Molecular Simulation: From Algorithms to Applications*, Academic Press, London, 2002.
- [6] K. Binder, D. W. Heermann, *Monte Carlo Simulation in Statistical Physics*, Springer-Verlag, Heidelberg, 1992.
- [7] D. P. Landau, K. Binder, *A Guide to Monte Carlo Simulation in Statistical Physics*, 2nd ed., Cambridge University Press, Cambridge, 2005.
- [8] R. H. Swendsen, J. S. Wang, *Phys. Rev. Lett.* 58 (1987) 86; U. Wolff, *Phys. Rev. Lett.* 62 (1989) 361.
- [9] B. A. Berg, T. Neuhaus, *Phys. Lett. B* 267 (1991) 249; *ibid*, *Phys. Rev. Lett.* 68 (1992) 9.
- [10] F. Wang, D. P. Landau, *Phys. Rev. Lett.* 86 (2001) 2050; *Phys. Rev. E* 64 (2001) 056101.
- [11] K. Hukushima, K. Nemoto, *J. Phys. Soc. Jpn.* 65 (1996) 1604; C. J. Geyer, *Markov-Chain Monte Carlo maximum Likelihood*, p. 156, *Comp. Sci. and Stat.* (1991).
- [12] E. Marinari, G. Parisi, *Europhys. Lett.* 19 (1992) 451.
- [13] D. J. Earl, M. W. Deem, *Phys. Chem. Chem. Phys.* 7 (2005) 3910; S. Singh, M. Chopra, J. J. de Pablo, *Annu. Rev. Chem. Biomol. Eng.* 3 (2012) 369.
- [14] C. E. Fiore, M. G. E. da Luz, *Phys. Rev. E* 82 (2010) 031104.
- [15] S. Park, V. S. Pande, *Phys. Rev. E* 76 (2007) 016703.
- [16] S. Park, *Phys. Rev. E* 77 (2008) 016709.
- [17] X. Huang, G. R. Bowmann, V. S. Pande, *J. Chem. Phys.* 128 (2008) 205106.
- [18] C. Zhang, J. P. Ma, *J. Chem. Phys.* 129 (2008) 134112.
- [19] T. Neuhaus, J. S. Hager, *Phys. Rev. E* 74 (2006) 036702.
- [20] T. Neuhaus, M. P. Magiera, U. H. E. Hansmann, *Phys. Rev. E* 76 (2007) 045701(R).
- [21] J. Kim, T. Keyes, J. E. Straub, *J. Chem. Phys.* 132 (2010) 224107.
- [22] J. Kim, J. E. Straub, T. Keyes, *J. Phys. Chem. B* 116 (2012) 8646.
- [23] Q. Lu, J. Kim, J. E. Straub, *J. Phys. Chem. B* 116 (2012) 8654.
- [24] Q. Lu, J. Kim, J. E. Straub, *J. Chem. Phys.* 138 (2013) 104119.
- [25] J. Kim, J. E. Straub, *J. Chem. Phys.* 133 (2010) 154101.
- [26] T. Nagai, Y. Okamoto, *Phys. Rev. E* 86 (2012) 056705.
- [27] D. Sabo, M. Meuwly, D. L. Freeman, J. D. Doll, *J. Chem. Phys.* 128 (2008) 174109.
- [28] C. E. Fiore, *J. Chem. Phys.* 135 (2011) 114107.
- [29] C. E. Fiore, M. G. E. da Luz, *J. Chem. Phys.* 133 (2010) 104904.
- [30] S. Koch, *Dynamics of First Order Phase Transitions in Equilibrium and Nonequilibrium Systems*, *Lectures Notes in Physics* 207, Springer-Verlag, New York, 1984; R. E. Kunz, *Dynamics of First-Order Phase Transitions in Mesoscopic and Macroscopic Equilibrium and Nonequilibrium Systems*, H. Deutsch Verlag, Frankfurt, 1995; P. Papon, J. Leblond, P. H. E. Meijer, *The Physics of Phase Transitions: Concepts and Applications*, 2nd ed., Springer, Heidelberg, 2010.
- [31] P. H. Nguyen, Y. Okamoto, P. Derreumaux, *J. Chem. Phys.* 138 (2013) 061102.
- [32] R. A. Sauerwein, M. J. de Oliveira, *Phys. Rev. B* 52 (1995) 3060.
- [33] C. E. Fiore, C. E. I. Carneiro, *Phys. Rev. E* 76 (2007) 021118.
- [34] C. E. Fiore, M. G. E. da Luz, *Phys. Rev. Lett.* 107 (2011) 230601.
- [35] C. E. Fiore, M. G. E. da Luz, *J. Chem. Phys.* 138 (2013) 014105.
- [36] For a given \mathcal{T}_R , contrary to the PT, in the ST just to consider non-adjacent exchanges does not necessary improve the protocol efficiency.
- [37] C. Predescu, M. Predescu, C. Ciobanu, *J. Chem. Phys.* 120 (2004) 4119; *J. Phys. Chem. B* 109 (2005) 4189.
- [38] A. Kone, D. A. Kofke, *J. Chem. Phys.* 122 (2005) 206101.
- [39] One way to define T_R , when no other procedure is available, is to apply simple Metropolis algorithms to successive temperatures above T_1 , picking the lowest one T for which the method is capable to give satisfactory results for that T .
- [40] F. Calvo, *J. Chem. Phys.* 123 (2005) 124106.
- [41] D. A. Kofke, *J. Chem. Phys.* 117 (2002) 6911.
- [42] M. Blume, V. J. Emery, R. B. Griffiths, *Phys. Rev. A* 4 (1971) 1071; W. Hoston, A. N. Berker, *Phys. Rev. Lett.* 67 (1991) 1027.
- [43] C. E. Fiore, M. M. Szortyka, M. C. Barbosa, V. B. Henriques, *J. Chem. Phys.* 131 (2009) 164506.
- [44] M. M. Szortyka, C. E. Fiore, V. B. Henriques, M. C. Barbosa, *J. Chem. Phys.* 133 (2010) 104904.
- [45] M. M. Szortyka, C. E. Fiore, V. B. Henriques, M. C. Barbosa, *Phys. Rev. E* 86 (2012) 031503.
- [46] G. M. Bell, D. A. Lavis, *J. Phys. A* 3 (1970) 568.
- [47] F. Y. Wu, *Rev. Mod. Phys.* 54 (1982) 235.
- [48] C. Tsallis, *J. Stat. Phys.* 52 (1988) 479.
- [49] N. Rathore, M. Chopra, J. J. de Pablo, *J. Chem. Phys.* 122 (2005) 024111.